Crystal structure of calcium L-5-methyltetrahydrofolate trihydrate type I, $C_{20}H_{23}N_7O_6Ca(H_2O)_3$

James A. Kaduk,[1,2,a] Nilan V. Patel,[3] and Joseph T. Golab[3]
[1]*Illinois Institute of Technology, 3101 S. Dearborn St., Chicago, IL 60616, USA*
[2]*North Central College, 131 S. Loomis St., Naperville, IL 60540, USA*
[3]*Illinois Mathematics and Science Academy, 1500 Sullivan Rd., Aurora, IL 60506-1000, USA*

(Received 23 January 2023; accepted 30 June 2023)

The crystal structure of L-5-methyltetrahydrofolate calcium trihydrate has been solved and refined using synchrotron X-ray powder diffraction data and optimized using density functional techniques. Calcium levomefolate trihydrate crystallizes in space group $P2_12_12_1$ (#19) with $a = 7.1706(6)$, $b = 6.5371(5)$, $c = 53.8357(41)$ Å, $V = 2523.58(26)$ Å^3, and $Z = 4$. The structure is characterized by alternating hydrophobic and hydrophilic layers along the *c*-axis. The Ca cations are 7-coordinate, and share edges to form chains along the *b*-axis. Each of the water molecules acts as a donor in two hydrogen bonds. The coordinated water molecule makes two strong intermolecular O–H···O hydrogen bonds to carboxyl and carbonyl groups. The two zeolitic water molecules form weaker hydrogen bonds, to carbonyl O atoms, ring N atoms, and aromatic C atoms. Several N–H···O/N hydrogen bonds, as well as C–H···O hydrogen bonds, also contribute to the lattice energy.

[doi:10.1017/S0885715623000246]

Key words: levomefolate calcium, Metafolin, Rietveld refinement, density functional theory

I. INTRODUCTION

Levomefolic acid is a metabolite of folic acid (Vitamin B9) and is a major active form of folate found in foods and in the blood circulation. It is transported across membranes, including the blood–brain barrier, and plays an essential role in DNA and protein synthesis. Levomefolate is approved as a food additive and is designated as a GRAS (generally recognized as safe) compound. It is available commercially as a crystalline Ca salt (trade name Metafolin), which has the required stability for use as a supplement (https://www.drugbank.ca/salts/DBSALY001276). The IUPAC name (CAS Registry number 151533-22-1 for the anhydrous salt) is (2S)-2-[[4-[[(6S)-2-amino-5-methyl-4-oxo-3,6,7,8-tetrahydropteridin-6-yl]methylamino]benzoyl]amino]pentanedioate calcium trihydrate. A two-dimensional molecular diagram is shown in Figure 1.

Stable crystalline salts of 5-methyltetrahydrofolic acid are disclosed and claimed in US Patent 6,441,168 (Müller et al., 2002; Eprova AG). The patent includes claims for "a water of crystallization of at least one equivalent per equivalent of 5-methyltetrahydrofolic acid" and "≥3 equivalents of water". Commercial samples are generally described as the trihydrate, although the pentahydrate is also available commercially. Powder diffraction data for additional (6S)-5-methyltetrahydrofolate calcium salts are reported in Chinese Patent CN 104530051 A (Wang and Cheng, 2015; Beijing Jinkang Hexin Pharmaceutical Technology Co.). A connectivity search in the Cambridge Structural Database (Groom et al., 2016) for derivatives of levomefolic acid yielded no hits. Name and formula searches in the Powder Diffraction File (Gates-Rector and Blanton, 2019) yielded no hits.

II. EXPERIMENTAL

Calcium L-5-methyltetrahydrofolate trihydrate (Lot #WN02-130227) was supplied by Virtus Pharmaceuticals. A laboratory pattern (measured on a Bruker D2 Phaser using Cu Kα radiation; $K_{\alpha1} = 1.540593$ Å, $K_{\alpha2} = 1.544451$ Å) could be indexed on a primitive monoclinic unit cell with $a = 13.314(3)$, $b = 26.868(6)$, $c = 8.187(2)$ Å, $\beta = 94.33(2)°$, $V = 2563.6(8)$ Å^3, and $Z = 4$. This cell predicted a peak at 3.3° 2θ, which was confirmed by changing the configuration of the diffractometer. Attempts to solve the structure using this cell were unsuccessful.

The same pale yellow powder was packed into a 1.5 mm diameter Kapton capillary, and rotated during the measurement at ~50 Hz. The powder pattern was measured at 295 K at beamline 11-BM (Antao et al., 2008; Lee et al., 2008; Wang et al., 2008) of the Advanced Photon Source at Argonne National Laboratory using a wavelength of 0.413691(2) Å from 0.5° to 50° 2θ with a step size of 0.001° and a counting time of 0.1 s/step. The high-resolution powder diffraction data were collected using twelve silicon crystal analyzers that allow for high angular resolution, high

[a]Author to whom correspondence should be addressed. Electronic mail: kaduk@polycrystallography.com

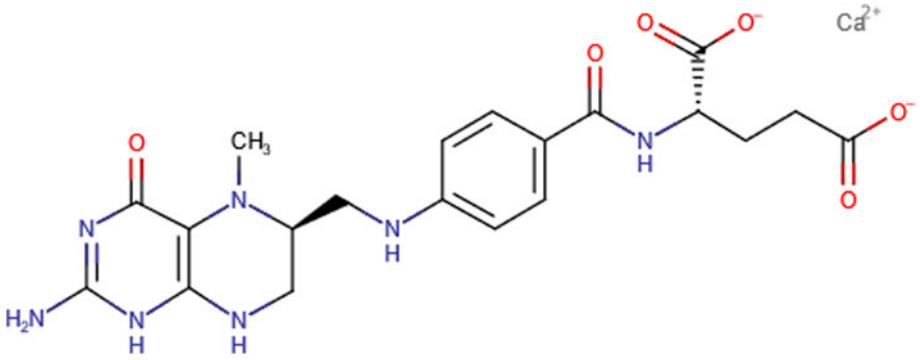

Figure 1. The 2D molecular structure of calcium L-5-methyltetrahydrofolate.

precision, and accurate peak positions. A mixture of silicon (NIST SRM 640c) and alumina (NIST SRM 676a) standards (ratio Al_2O_3:Si = 2:1 by weight) was used to calibrate the instrument and refine the monochromatic wavelength used in the experiment.

The synchrotron pattern was indexed with difficulty using DICVOL14 (Louër and Boultif, 2014) on a primitive monoclinic unit cell having $a = 6.9575$, $b = 6.5372$, $c = 53.7699$ Å, $\beta = 92.320°$, $V = 2444.33$ Å^3, and $Z = 4$. Analysis of the systematic absences using EXPO2014 (Altomare et al., 2013) suggested the space group $P2_1$. Attempts to solve the structure using this cell yielded some plausible structures, but they all contained some molecular overlap. Analysis of this cell using PLATON (Spek, 2009, 2020) showed that it was not the conventional monoclinic cell, which has $a = 7.202$, $b = 6.548$, $c = 53.837$ Å, and $\beta = 90.5\ 4°$. The fact that the β angle was close to 90° suggested that we explore orthorhombic unit cells. EXPO2014 yielded a better Le Bail fit using an orthorhombic cell, and suggested the space group $P2_12_12_1$, which has a 4-fold general position. A reduced cell search in the Cambridge Structural Database (Groom et al., 2016) yielded 36 hits, but no folate derivatives.

The levomefolic acid molecule was downloaded from PubChem (Kim et al., 2023) as Conformer3D_CID_135398561.mol2. In this molecule, both C14 and C25 have the *S* stereochemistry. The structure was difficult to solve, using several different strategies and programs. The successful solution came by using FOX (Favre-Nicolin and Černý, 2002). The maximum $\sin\theta/\lambda$ used was 0.25 Å^{-1}. The anion (converted to a Fenske-Hall *Z*-matrix using OpenBabel (O'Boyle et al., 2011)), a Ca atom, and 3 O atoms (for the water molecules) were used as fragments, along with 001 preferred orientation (the extreme anisotropy of the unit cell makes preferred orientation likely) and a bump penalty (which increases the cost factor when pairs of atoms become closer than specified distances). In the lowest-cost solution, two of the O atoms were too close to each other, so one was removed from the model. The third O was added in a void, detected by Mercury (Macrae et al., 2020). The default mode of FOX includes enough molecular flexibility to invert the chirality of a carbon atom occasionally, as was the case here. In the lowest-cost model, C25 was R, so H47 was removed and reintroduced to the other side of this C atom using Materials Studio (Dassault, 2021). This model was subjected to a molecular mechanics optimization (fixed unit cell) using the Forcite module of Materials Studio. This optimized model was the start of a DFT optimization using CRYSTAL14 (Dovesi et al., 2018). The basis sets for the H, C, N, and O atoms were those of Gatti et al. (1994), and the basis set for Ca was that of Peintinger et al. (2013). The calculation was run on eight 2.1 GHz Xeon cores (each with 6 GB RAM) of a 304-core Dell Linux cluster at IIT, using 8 *k*-points and the B3LYP functional, and took ~150 h.

Rietveld refinement was carried out using GSAS-II (Toby and Von Dreele, 2013). Only the 0.7–18.0° portion of the diffraction pattern was included in the refinement (d_{min} = 1.322 Å). All non-H bond distances and angles in the folate anion were subjected to restraints, based on a Mercury/Mogul Geometry Check (Bruno et al., 2004; Sykes et al., 2011) of the molecule. The Mogul average and standard deviation for each quantity were used as the restraint parameters. The Ca–O distances were restrained manually at 2.48(10) Å. The restraints contributed 6.87% to the overall χ^2. The hydrogen atoms were included in calculated positions, which were recalculated during the refinement using Materials Studio. The U_{iso} were grouped by chemical similarity, and the U_{iso} of each H atom was constrained to be 1.3× that of the heavy atom to which it is attached. The background was modeled using a 6-term shifted Chebyshev polynomial, along with one peak at 4.56° to model the scattering from the Kapton capillary and an amorphous component. The peak for the Kapton capillary generally occurs ~5.2°.

The final refinement of 136 variables using 17 303 observations and 91 restraints yielded the residuals $R_{wp} = 0.1011$ and GOF = 1.77. The largest peak (0.06 Å from Ca34) and hole (1.82 Å from C21) in the difference Fourier map were 0.17 and −0.12(3) eÅ^{-3}, respectively. The largest errors in the fit (Figure 2) are in the shapes of some of the peaks. The data did not support refinement of the generalized microstrain model, so a uniaxial model (with 001) as the unique axis was used.

Additionally, a dihydrate model (without a coordinated water molecule, and derived from an optimization using VASP (Kresse and Furthmüller, 1996)) was refined. This model yielded poorer residuals: $R_{wp} = 0.1252$ and GOF = 2.13.

III. RESULTS AND DISCUSSION

This synchrotron power pattern of calcium L-5-methyltetrahydrofolate trihydrate is in excellent agreement with that reported by Müller et al. (2002) (Figure 3). The agreement is good enough to conclude that the patterns represent the

https://doi.org/10.1017/S0885715623000246 Published online by Cambridge University Press

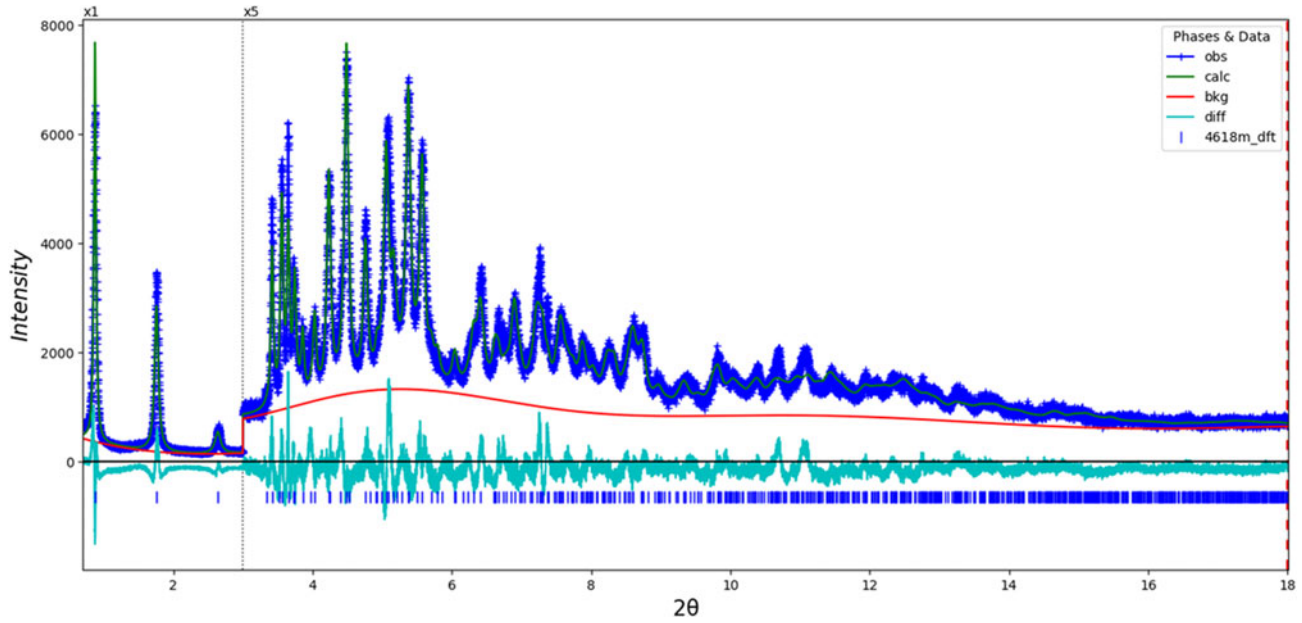

Figure 2. The Rietveld plot for the refinement of calcium L-5-methyltetrahydrofolate trihydrate. The blue crosses represent the observed data points, and the green line is the calculated pattern. The cyan curve is the error plot, and the red line is the background curve. The vertical scale has been multiplied by a factor of 5× for $2\theta > 3.0°$.

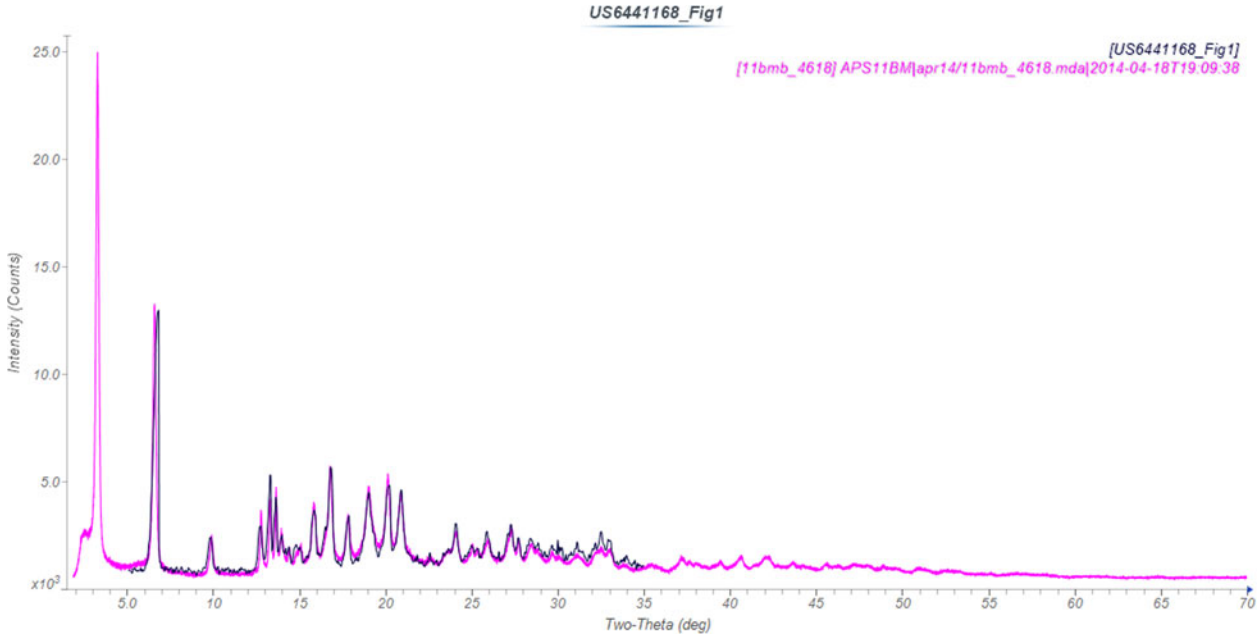

Figure 3. Comparison of the synchrotron pattern of calcium L-5-methyltetrahydrofolate trihydrate (magenta) to that of Form I reported by Müller et al. (2002; black). Note that the patent pattern does not include the lowest-angle (and strongest) peak of the pattern. The literature pattern (measured using Cu K_α radiation) was digitized using UN-SCAN-IT (Silk Scientific, 2013) and converted to the synchrotron wavelength of 0.458963(2) Å using JADE Pro (MDI, 2022). Image generated using JADE Pro (MDI, 2022).

same material, known as Type I. We should note that the patent pattern does not include the strongest peak of the pattern, because the pattern was not measured to low-enough an angle. This is not a problem for characterizing the phase for patent purposes, but is a useful cautionary tale.

The refined atom coordinates of L-5-methyltetrahydrofolate trihydrate Type I and the coordinates from the DFT optimization are reported in the CIFs deposited with ICDD. The root-mean-square (rms) Cartesian displacement of the non-hydrogen atoms in the Rietveld-refined and DFT-optimized structures is 0.744 Å (Figure 4), outside the normal range for correct structures (van de Streek and Neumann, 2014). The absolute difference in the Ca position in the two structures is 1.025 Å. The major differences are in the orientation of the C21–C29 phenyl ring, the orientations of the side chains, and the absolute position of the molecule in the unit cell. In the population of samples of this compound, this is an exceptionally crystalline one (hence the progress described here), but the peaks are relatively broad and the sample contains an amorphous component. As we will see later, the sample

https://doi.org/10.1017/S0885715623000246 Published online by Cambridge University Press

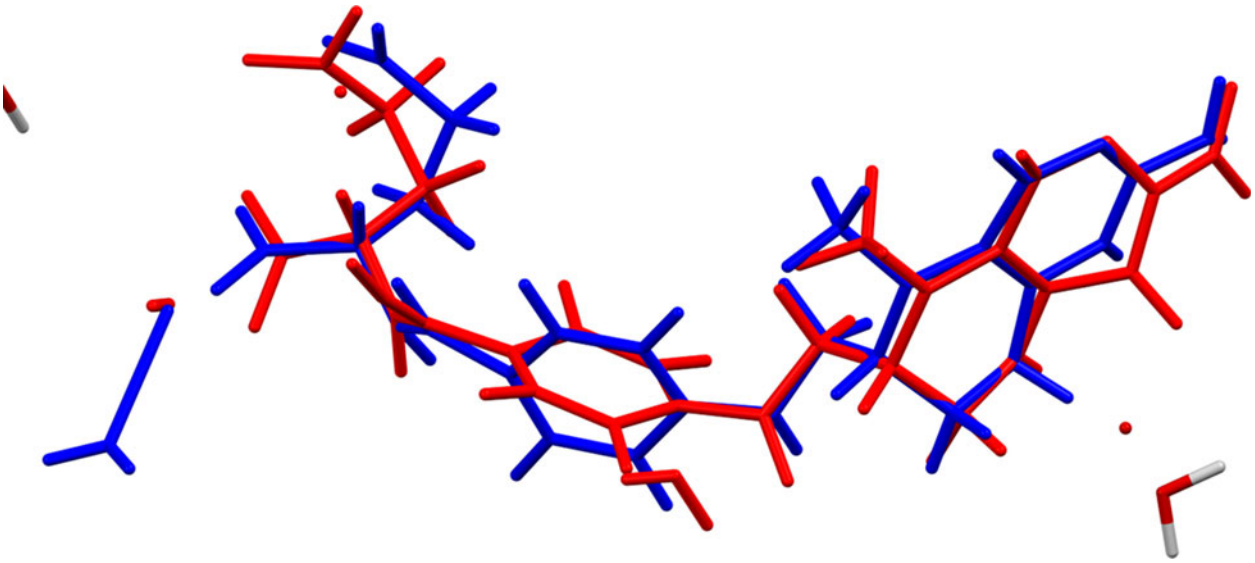

Figure 4. Comparison of the Rietveld-refined (red) and VASP-optimized (blue) structures of calcium L-5-methyltetrahydrofolate trihydrate. The rms Cartesian displacement is 0.744 Å. Image generated using Mercury (Macrae et al., 2020).

exhibits significant texture. All of these "features" mean that we can expect poorer accuracy of the refined structure than usual. Perhaps this should be considered a "proposed" structure for this compound; it is certainly better than no structure. The discussion below concentrates on the DFT-optimized structure, as we believe it is more reliable. The asymmetric unit (with atom numbering) is illustrated in Figure 5, and the crystal structure is presented in Figure 6.

The structure is characterized by alternating hydrophobic and hydrophilic layers along the *c*-axis (Figure 6). The Ca cations are 7-coordinate (one water molecule and six carboxylate oxygen atoms), and share edges to form chains along the *b*-axis (Figure 7). The bond valence sum of the Ca is 1.89. As expected, the carboxylate groups bind to the Ca. The group C32–O3–O4 bridges two Ca34, while the group C33–O5–O6 chelates to one Ca34, and bridges two others. One water molecule (O35) is coordinated to the Ca, while the other two (O36 and O37) are zeolitic. Additional small voids can be located by decreasing the probe radius in Mercury to 1.0 Å (from the default value of 1.2 Å) (Figure 8). The presence of additional water molecules in some samples can thus be rationalized easily. Attempts to refine the occupancies of water molecules placed in these voids resulted in values insignificantly different from zero, consistent with the formulation as a trihydrate.

Thermogravimetric analysis (TGA) indicated that the sample was a hexahydrate. The TGA, however, was measured 5 years after the sample had been acquired and the synchrotron pattern measured, so it is uncertain how relevant that water content is to the specimen used to measure the data. At the time of this writing, the diffraction pattern of the sample differed from the synchrotron pattern, indicating that the sample changed over time. Comparison of the DFT-optimized trihydrate and dihydrate structures (Figure 9) reveals significant

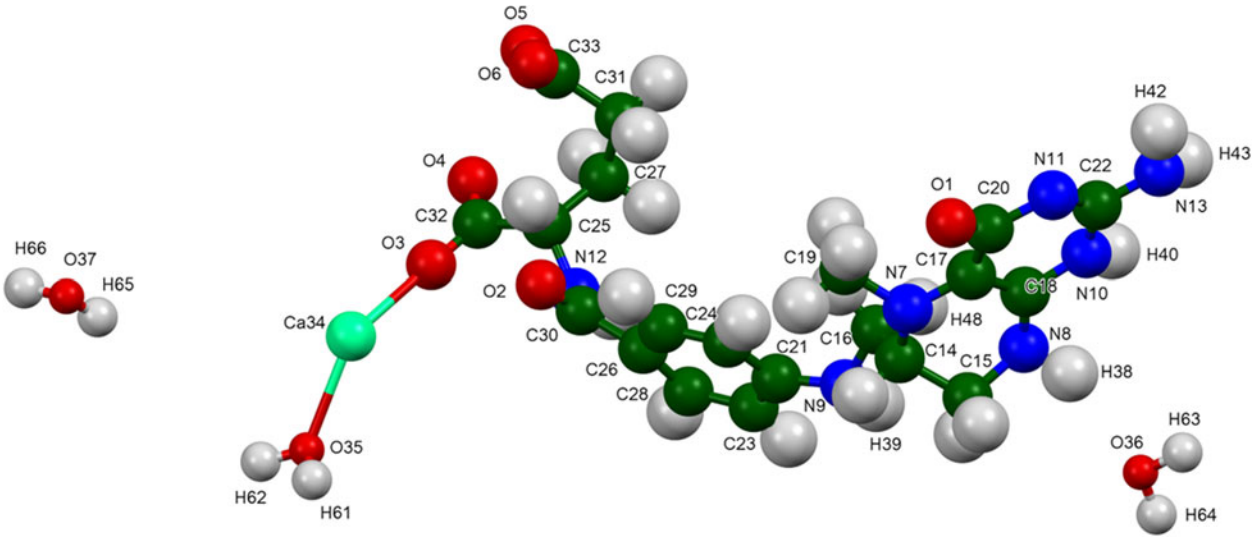

Figure 5. The asymmetric unit of calcium L-5-methyltetrahydrofolate trihydrate, with the atom numbering. The atoms are represented by 50% probability spheroids/ellipsoids. Image generated using Mercury (Macrae et al., 2020).

https://doi.org/10.1017/S0885715623000246 Published online by Cambridge University Press

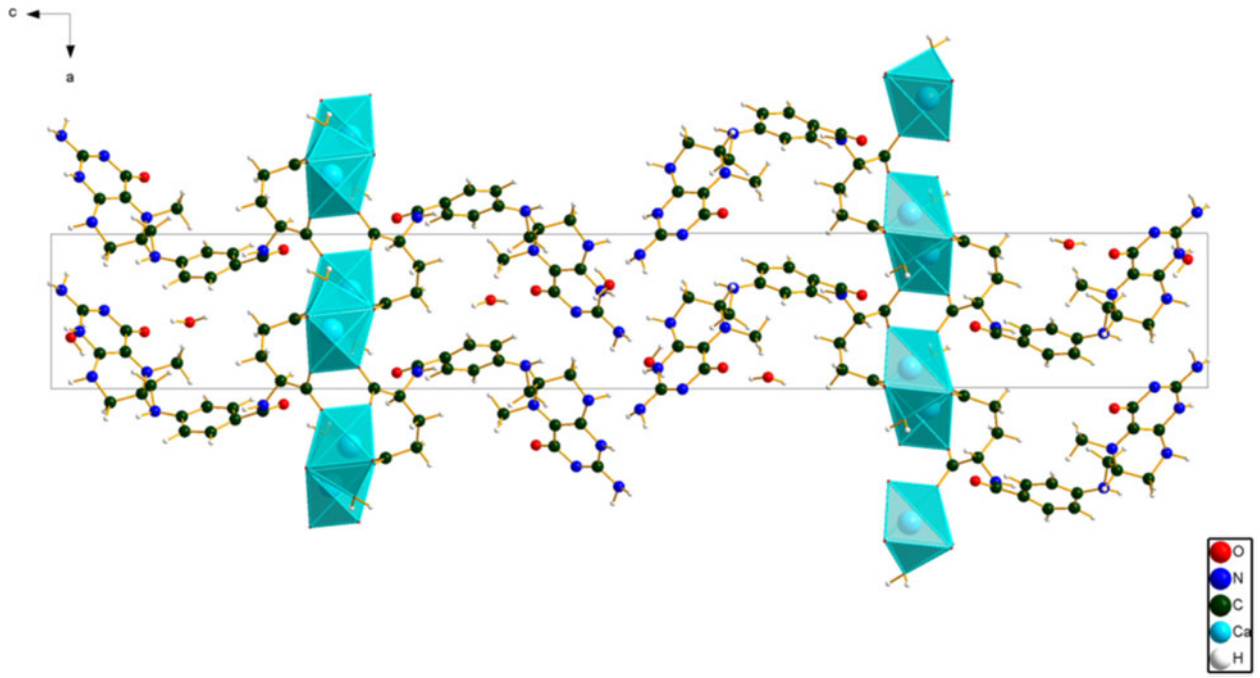

Figure 6. The crystal structure of calcium L-5-methyltetrahydrofolate trihydrate, viewed down the *b*-axis. Image generated using Diamond (Crystal Impact, 2022).

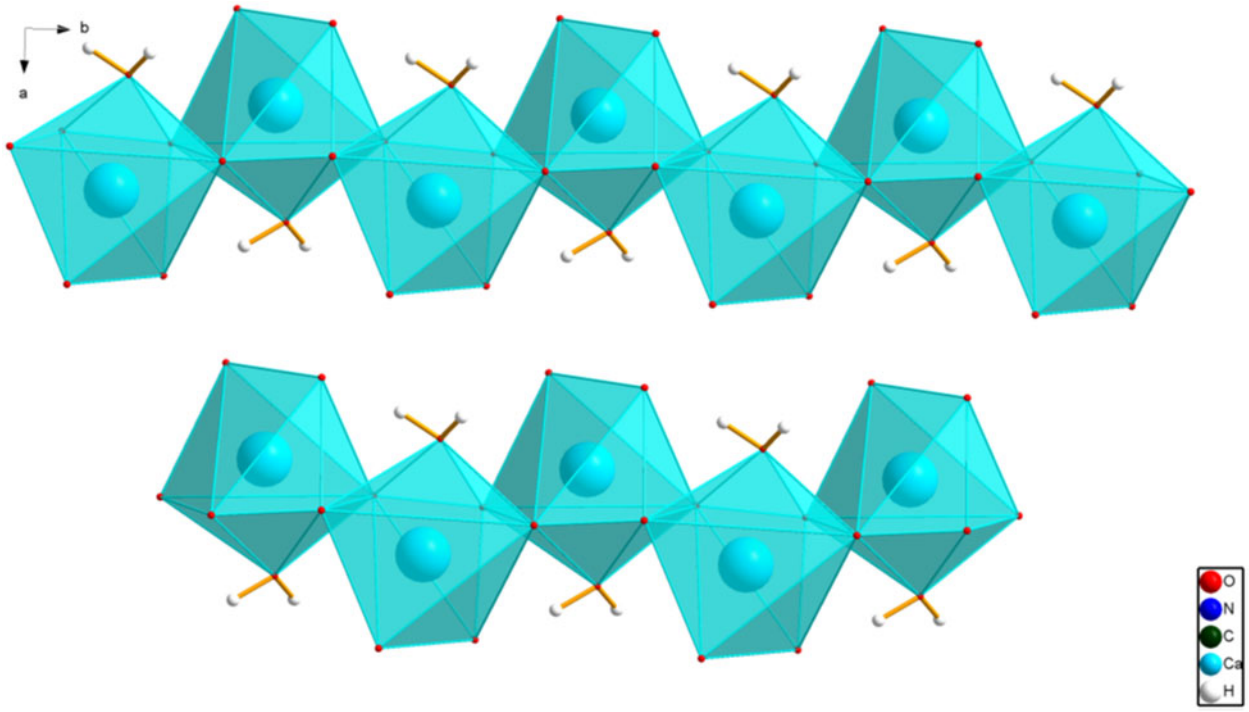

Figure 7. The chains of edge-sharing CaO_7 coordination polyhedra, viewed down the *c*-axis. Image generated using Diamond (Crystal Impact, 2022).

differences. The water content can apparently affect the structure significantly, perhaps resulting in the poorer-than-usual agreement of the refined and optimized structures.

Almost all of the bond distances, angles, and torsion angles fall within the normal ranges indicated by a Mercury/Mogul Geometry check (Macrae et al., 2020). The O57–C28–C30 angle of 109.3° (average = 105.8(10)°, *Z*-score = 3.6) is flagged as unusual. This angle lies slightly outside a narrow distribution of a few similar angles. The torsion angle C9–O54–C11–C12 is flagged as unusual; this represents the linking of the two portion of the molecule, and it is likely that crystal packing forces influence the molecular conformation. The torsion angles involving rotation around the C37–C38 bond (such as C33–C37–C38–C39) are flagged as

https://doi.org/10.1017/S0885715623000246 Published online by Cambridge University Press

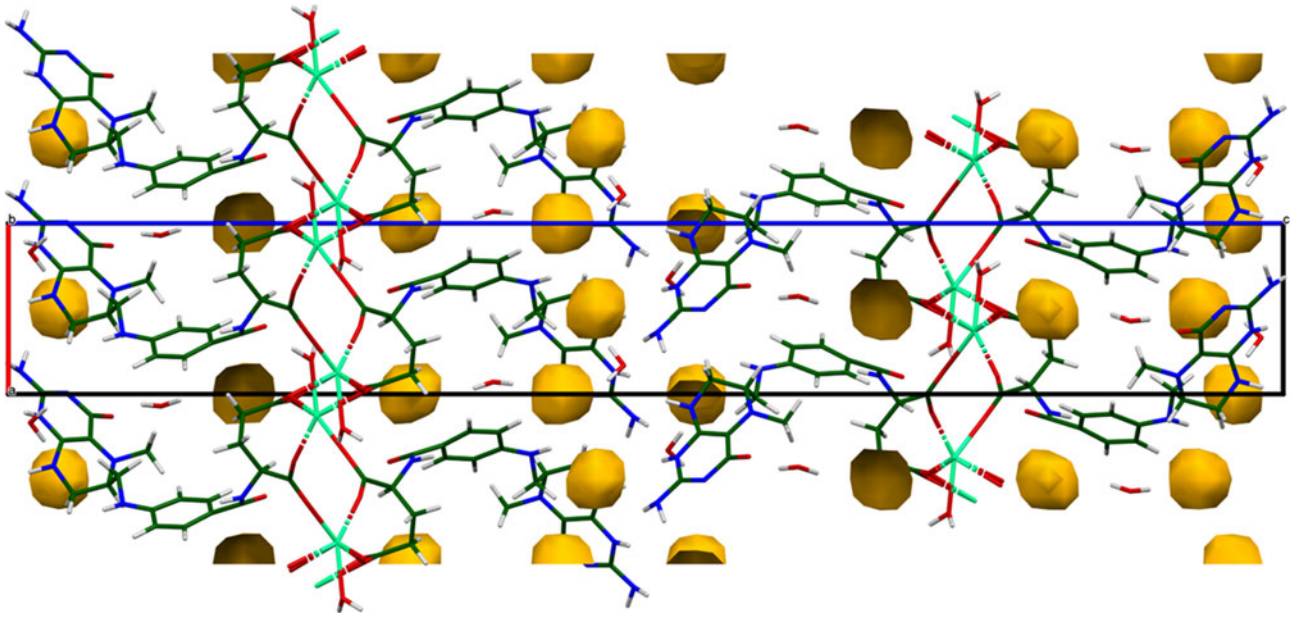

Figure 8. Potential additional voids in the crystal structure of calcium L-5-methyltetrahydrofolate trihydrate, obtained by decreasing the probe radius to 1.0 Å. Image generated using Mercury (Macrae et al., 2020).

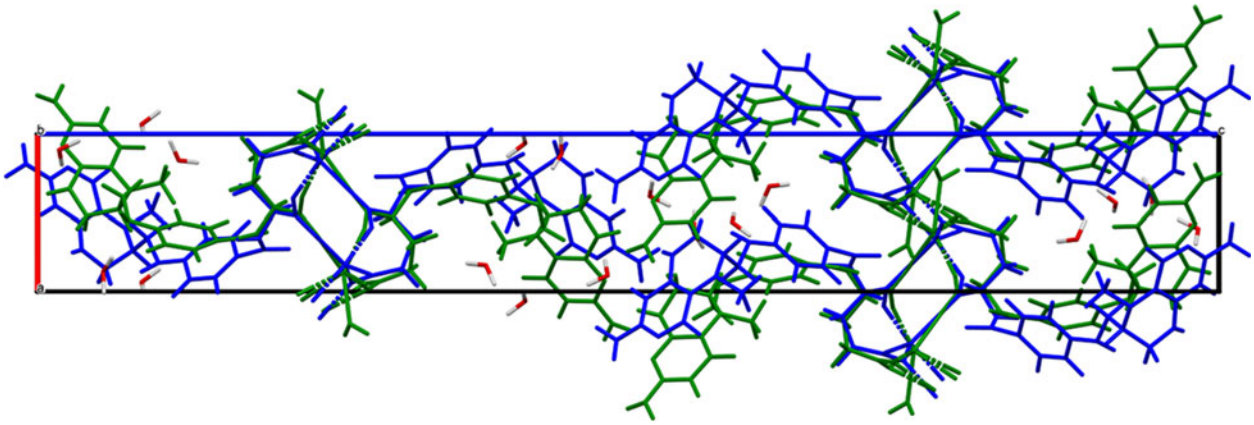

Figure 9. Comparison of the DFT-optimized crystal structure of calcium L-5-methyltetrahydrofolate trihydrate (blue) to that of the dihydrate (green). Image generated using Mercury (Macrae et al., 2020).

unusual. This angle lies near a minor *gauche* population of mainly *trans* angles.

Quantum chemical geometry optimization of the isolated anion (DFT/B3LYP/6-31G*/water) using Spartan '18 (Wavefunction, 2020) indicated that the observed conformation of the cation is 36.5 kcal/mol higher in energy than the local minimum conformation. The conformational differences are spread throughout the molecule. The global minimum-energy conformation of the anion (MMFF force field) curls up on itself so that the ring systems are roughly parallel, and intramolecular N–H···O hydrogen bonds form between the amino group N13 and carboxylate oxygen atoms. Intermolecular interactions are thus important in determining the solid-state conformation.

Analysis of the contributions to the total crystal energy of the structure using the Forcite module of Materials Studio (Dassault Systèmes, 2021) suggests that angle distortion terms dominate the intramolecular deformation energy, but that bond and torsion distortion terms are also significant. The intermolecular energy is dominated by electrostatic attractions, which in this force field analysis also include hydrogen bonds. The hydrogen bonds are better analyzed using the results of the DFT calculation.

Hydrogen bonds are prominent in the crystal structure (Table I). Each of the water molecules acts as a donor in two hydrogen bonds. The coordinated water molecule O35 makes two strong intermolecular O–H···O hydrogen bonds to carboxyl and carbonyl groups. The zeolitic water molecules O36 and O37 form weaker hydrogen bonds, to carbonyl O atoms, ring N atoms, and aromatic C atoms. Several N–H···O/N hydrogen bonds, as well as C–H···O hydrogen bonds, also contribute to the lattice energy. The energies of the O–H···O hydrogen bonds were calculated using the correlation of Rammohan and Kaduk (2018), and the energies of the N–H···O hydrogen bonds were calculated using the correlation of Wheatley and Kaduk (2019).

https://doi.org/10.1017/S0885715623000246 Published online by Cambridge University Press

TABLE I. Hydrogen bonds (CRYSTAL14) in calcium L-5-methyltetrahydrofolate trihydrate Type I.

H-Bond	D-H (Å)	H···A (Å)	D···A (Å)	D-H···A (°)	Overlap (*e*)	E (kcal/mol)
O37–H66···O1	0.983	1.775	2.755	175.2	0.057	13.0
O37–H65···C24	0.967	2.585	3.392	141.1	0.014	
O36–H64···N8	0.991	1.757	2.745	174.4	0.064	
O36–H63···N11	0.966	2.338	3.012	126.3	0.012	
O35–H62···O2	0.975	1.741	2.708	171.1	0.046	11.7
O35–H61···O3	0.980	1.826	2.751	156.2	0.048	12.0
N13–H43···O36	1.019	1.878	2.839	155.7	0.063	5.8
N13–H42···N10	1.008	2.563	2.918	100.3	0.010	
N11–H40···N9	1.024	2.379	3.350	157.9	0.037	
N9–H39···N7	1.019	2.364	3.278	148.7	0.030	
N8–H38···O36	1.023	2.152	3.045	144.7	0.036	4.4
C29–H58···O2	1.084	2.287[a]	2.693	99.9	0.019	
C27–H55···O4	1.091	2.228[a]	2.765	107.8	0.026	
C25–H54···O2	1.095	2.316[a]	2.829	106.5	0.017	
C24–H53···C19	1.075	2.410[a]	3.480	173.3	0.011	
C19–H51···O37	1.096	2.452	3.341	137.3	0.019	
C19–H49···O1	1.086	2.051[a]	2.837	126.7	0.024	
C16–H48···O1	1.092	2.590			0.019	

[a]Intramolecular.

The Bravais–Friedel–Donnay–Harker (Bravais, 1866; Friedel, 1907; Donnay and Harker, 1937) morphology suggests that we might expect platy morphology for calcium L-5-methyltetrahydrofolate trihydrate, with {002} as the principal faces. A sixth-order spherical harmonic model was included in the refinement. The refined texture index was 1.563(10), indicating that preferred orientation was significant in this rotated capillary specimen. We should expect that preferred orientation would be significant in most specimens of this material, especially on a Bragg-Brentano diffractometer.

IV. DEPOSITED DATA

The Crystallographic Information Framework (CIF) files containing the results of the Rietveld refinement (including the raw data) and the DFT geometry optimization were deposited with the ICDD. The data can be requested at pdj@icdd.com.

ACKNOWLEDGEMENTS

The use of the Advanced Photon Source at Argonne National Laboratory was supported by the U.S. Department of Energy, Office of Science, Office of Basic Energy Sciences, under Contract No. DE-AC02-06CH11357. We thank Lynn Ribaud and Saul Lapidus for their assistance in the data collection, Andrey Rogachev for the use of computing resources at IIT, and Rhett Daniels of Virtus Pharmaceuticals for the sample.

CONFLICTS OF INTEREST

The authors have no conflicts of interest to declare.

REFERENCES

Altomare, A., C. Cuocci, C. Giacovazzo, A. Moliterni, R. Rizzi, N. Corriero, and A. Falcicchio. 2013. "EXPO2013: A Kit of Tools for Phasing Crystal Structures from Powder Data." *Journal of Applied Crystallography* 46: 1231–35.

Antao, S. M., I. Hassan, J. Wang, P. L. Lee, and B. H. Toby. 2008. "State-of-the-Art High-Resolution Powder X-ray Diffraction (HRPXRD) Illustrated with Rietveld Refinement of Quartz, Sodalite, Tremolite, and Meionite." *Canadian Mineralogist* 46: 1501–09.

Bravais, A. 1866. *Etudes Cristallographiques*. Paris, Gauthier Villars.

Bruno, I. J., J. C. Cole, M. Kessler, J. Luo, W. D. S. Motherwell, L. H. Purkis, B. R. Smith, R. Taylor, R. I. Cooper, S. E. Harris, and A. G. Orpen. 2004. "Retrieval of Crystallographically-Derived Molecular Geometry Information." *Journal of Chemical Information and Computer Sciences* 44: 2133–44.

Crystal Impact - Dr. H. Putz & Dr. K. Brandenburg. 2022. Diamond - Crystal and Molecular Structure Visualization. Kreuzherrenstr. 102, 53227 Bonn, Germany. https://www.crystalimpact.de/diamond.

Dassault Systèmes. 2021. *Materials Studio 2021*. San Diego, CA, BIOVIA.

Donnay, J. D. H., and D. Harker. 1937. "A New Law of Crystal Morphology Extending the Law of Bravais." *American Mineralogist* 22: 446–47.

Dovesi, R., A. Erba, R. Orlando, C. M. Zicovich-Wilson, B. Civalleri, L. Maschio, M. Rérat, S. Casassa, J. Baima, S. Salustro, and B. Kirtman. 2018. "Quantum-Mechanical Condensed Matter Simulations with CRYSTAL." *Wiley Interdisciplinary Reviews: Computational Molecular Science* 8: e1360.

Favre-Nicolin, V., and R. Černý. 2002. "FOX, Free Objects for Crystallography: A Modular Approach to Ab Initio Structure Determination from Powder Diffraction.'" *Journal of Applied Crystallography* 35: 734–43.

Friedel, G. 1907. "Etudes sur la loi de Bravais." *Bulletin de la Société Française de Minéralogie* 30: 326–455.

Gates-Rector, S., and T. N. Blanton. 2019. "The Powder Diffraction File: A Quality Materials Characterization Database." *Powder Diffraction* 39: 352–60.

Gatti, C., V. R. Saunders, and C. Roetti. 1994. "Crystal-Field Effects on the Topological Properties of the Electron-Density in Molecular Crystals - The Case of Urea." *Journal of Chemical Physics* 101: 10686–96.

Groom, C. R., I. J. Bruno, M. P. Lightfoot, and S. C. Ward. 2016. "The Cambridge Structural Database." *Acta Crystallographica Section B: Structural Science, Crystal Engineering and Materials* 72: 171–79.

Kim, S., J. Chen, T. Cheng, A. Gindulyte, J. He, S. He, Q. Li, B. A. Shoemaker, P. A. Thiessen, B. Yu, L. Zaslavsky, J. Zhang, and E. E. Bolton. 2023. "PubChem 2023 update." *Nucleic Acids Research* 51 (D1): D1373–80. doi:10.1093/nar/gkac956.

Kresse, G., and J. Furthmüller. 1996. "Efficiency of Ab-Initio Total Energy Calculations for Metals and Semiconductors Using a Plane-Wave Basis Set." *Computational Materials Science* 6: 15–50.

Lee, P. L., D. Shu, M. Ramanathan, C. Preissner, J. Wang, M. A. Beno, R. B. Von Dreele, L. Ribaud, C. Kurtz, S. M. Antao, X. Jiao, and B. H. Toby. 2008. "A Twelve-Analyzer Detector System for High-

Resolution Powder Diffraction." *Journal of Synchrotron Radiation* 15: 427–32.

Louër, D., and A. Boultif. 2014. "Some Further Considerations in Powder Diffraction Pattern Indexing with the Dichotomy Method." *Powder Diffraction* 29: S7–12.

Macrae, C. F., I. Sovago, S. J. Cottrell, P. T. A. Galek, P. McCabe, E. Pidcock, M. Platings, G. P. Shields, J. S. Stevens, M. Towler, and P. A. Wood. 2020. "*Mercury 4.0*: From Visualization to Design and Prediction." *Journal of Applied Crystallography* 53: 226–35.

MDI. 2022. *JADE Pro Version 8.2*. Livermore, CA, Materials Data.

Müller, R., R. Moser, and T. Egger. 2002. "Stable Crystalline Salts of 5-Methyltetrahydrofolic Acid." US Patent 6,441,168 B1.

O'Boyle, N. M., M. Banck, C. A. James, C. Morley, T. Vandermeersch, and G. R. Hutchison. 2011. "Open Babel: An Open Chemical Toolbox." *Journal of Chemical Informatics* 3: 33. doi:10.1186/1758-2946-3-33.

Peintinger, M. F., D. Vilela Oliveira, and T. Bredow. 2013. "Consistent Gaussian Basis Sets of Triple-Zeta Valence with Polarization Quality for Solid-State Calculations." *Journal of Computational Chemistry* 34: 451–59.

Rammohan, A., and J. A. Kaduk. 2018. "Crystal Structures of Alkali Metal (Group 1) Citrate Salts." *Acta Crystallographica Section B: Crystal Engineering and Materials* 74: 239–52. doi:10.1107/S2052520618002330.

Silk Scientific. 2013. *UN-SCAN-IT 7.0*. Orem, UT, Silk Scientific Corporation.

Spek, A. L. 2009. "Structure Validation in Chemical Crystallography." *Acta Crystallographica D* 65: 148–55.

Spek, A. L. 2020. "CheckCIF Validation Alerts: What They Mean and How to Respond." *Acta Crystallographica E* 76: 1–11.

Sykes, R. A., P. McCabe, F. H. Allen, G. M. Battle, I. J. Bruno, and P. A. Wood. 2011. "New Software for Statistical Analysis of Cambridge Structural Database Data." *Journal of Applied Crystallography* 44: 882–86.

Toby, B. H., and R. B. Von Dreele. 2013. "GSAS II: The Genesis of a Modern Open Source All Purpose Crystallography Software Package." *Journal of Applied Crystallography* 46: 544–49.

van de Streek, J., and M. A. Neumann. 2014. "Validation of Molecular Crystal Structures from Powder Diffraction Data with Dispersion-Corrected Density Functional Theory (DFT-D)." *Acta Crystallographica Section B: Structural Science, Crystal Engineering and Materials* 70: 1020–32.

Wang, Z., and Y. Cheng. 2015. "Stable (6R,S)-5-methyl tetrahydrofolic acid crystal form and preparation method thereof." Chinese Patent CN 104530051 A.

Wang, J., B. H. Toby, P. L. Lee, L. Ribaud, S. M. Antao, C. Kurtz, M. Ramanathan, R. B. Von Dreele, and M. A. Beno. 2008. "A Dedicated Powder Diffraction Beamline at the Advanced Photon Source: Commissioning and Early Operational Results." *Review of Scientific Instruments* 79: 085105.

Wavefunction, Inc. 2020. Spartan '18. Version 1.4.5. Wavefunction Inc., 18401 Von Karman Ave., Suite 370, Irvine CA 96212.

Wheatley, A. M., and J. A. Kaduk. 2019. "Crystal Structures of Ammonium Citrates." *Powder Diffraction* 34: 35–43.